Modelling and Precalculation of Additional Losses of Inverter Fed Asynchronous Induction Machines of Traction Drives

Erich Schmidt, *Member*, *IEEE*
Institute of Energy Systems and Electric Drives
Vienna University of Technology, Vienna, Austria

Florian Müllner, Harald Neudorfer
Traktionssysteme Austria
Wiener Neudorf, Austria

***Abstract* – The evaluation of additional losses of inverter fed asynchronous induction machines with design and operation is an important task for many years. On the other hand, asynchronous induction machines used with traction drives of rail transportation vehicles have different design strategies compared against commonly used standard machines. Since such machines have a very high utilization additionally, accurate modelling and precalculation of the additional losses caused by the inverter are an important task with both tender phase as well as electromagnetic and thermal initial design of these machines. Thus, the main components of these additional losses are discussed based on the spectrum of the non-sinusoidal voltages supplied by the inverter. An important viewpoint of modelling and precalculation presented herein is given to the comparison with detailed measurements from different already built machines.**

***Index Terms* – Additional losses, Eddy current losses, Iron losses, Asynchronous machine, Induction machine**

I. Introduction

Additional losses of asynchronous induction machines utilized in traction drives caused by the inverter have a great impact on both electromagnetic and thermal behaviour of such machines [1]–[4]. Against industrial utilized machines, design and manufacturing cycles of these machines are mostly very different. Therefore, accurate modelling and pre-evaluation of the additional losses caused by the inverter are very important tasks in particular with tender phase and initial design. In these design phases, many details of both machine and inverter, in particular operating and switching strategies, have not been specified. Consequently, very detailed analysis methods such as multi-domain coupled finite element analyses are not advisable.

Instead, equivalent circuits of the induction machine for each higher harmonic component of the terminal voltages applied by the inverter are utilized to calculate the higher harmonic components of the current consumption. Subsequently, the iron and power losses are evaluated in dependence on the operating conditions particularly taking into account the various switching strategies of the inverter. Based on detailed measurement data from already built machines, a fast and reliable calculation method of the additional losses suitable for the initial design of new machines is presented.

II. Equivalent Circuits

As depicted in Fig. 1, the supplying voltage source inverter operates in either asynchronous or synchronous mode, in particular with higher fundamental frequencies. Regardless of the pulse pattern mode, the voltages applied to the machine and consequently the consumed currents are always non-sinusoidal with dominant fundamental harmonic components U_1, I_1 and various higher harmonic components U_k, I_k, $k = 1 + 6g$, $g \in \mathcal{Z}$. Based on Fourier series expansions of voltages and currents,

$$U(\omega t) = \sum_k \sqrt{2}\, U_k \, \mathrm{e}^{j\varphi_{uk}} \, \mathrm{e}^{jk\omega t} \ , \tag{1}$$

$$I(\omega t) = \sum_k \sqrt{2}\, I_k \, \mathrm{e}^{j\varphi_{ik}} \, \mathrm{e}^{jk\omega t} \ , \tag{2}$$

an equivalent circuit of each harmonic order k as depicted in Fig. 2 is introduced. The slip values s_k of the higher harmonics are obtained from the fundamental slip s_1 as

$$1 - s_1 = k\,(1 - s_k) \ . \tag{3}$$

With rated operational conditions, the fundamental slip $s_1 \ll 1$ causes slip values of the higher harmonics $s_k \approx 1$. Consequently, the higher harmonics will generate additional losses which are approximately independent of the actual operational point [1], [3]. The parameters of each equivalent circuit are further calculated according to the following suggestions about power and iron losses.

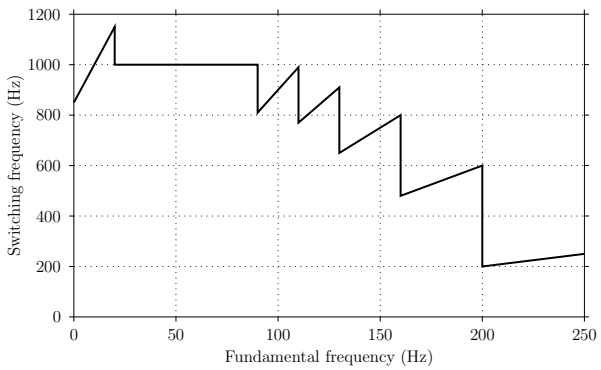

Fig. 1: Switching frequency versus fundamental frequency of a voltage source inverter of traction drives

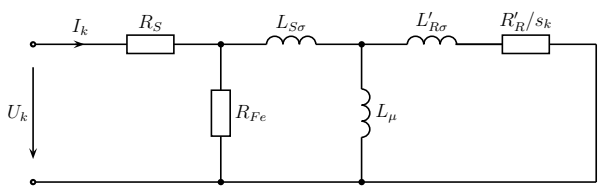

Fig. 2: Equivalent circuit for each harmonic component

III. Power Losses

The most important component of the additional losses concerned arises as power losses from higher current harmonics in the conductors of both stator and rotor windings [3]–[5]. Due to the high frequencies of these current components, the current displacement effects have to be considered in detail. Based on the well-known skin depth

$$\delta_C = \sqrt{\frac{2}{\omega \mu_0 \gamma}} \tag{4}$$

in dependence on circular frequency ω and conductivity γ [3], [4], [6], a reduced slot conductor height or radius ξ and additionally a complex parameter ζ are defined as

$$\xi = \frac{h_C}{\delta_C} \quad \text{or} \quad \xi = \frac{r_C}{\delta_C} \ , \quad \zeta = \xi\,(1+j) \ , \tag{5}$$

where h_C, r_C denote height or radius of the conductor. The skin effect significantly affects the impedance of slot conductors along the lengths of stator and rotor lamination stack. In particular with the stator, the current displacement within the end winding region has to be considered, too [3], [4].

A. Opened stator slots

Asynchronous induction machines of traction drives are always equipped with opened stator slots in order to carry the form-wound winding coils [7], [8]. Usually, there is an equal number of rectangular conductors in both upper and lower layers resulting in an even number n of slot conductors. By using DC resistance R_0 and DC inductance L_0 [6], the complex impedance of each of the n rectangular slot conductors is given by

$$\frac{Z(\zeta)}{R_0} = \zeta \left(\coth\zeta + 2p\,(p-1)\,\tanh\frac{\zeta}{2} \right) \ , \quad 1 \le p \le n \ , \tag{6}$$

whereby the insulation of the form-wound winding coils results in the modified reduced slot conductor height

$$\xi = \frac{h_C}{\delta_C}\sqrt{\frac{b_C}{b_S}} \tag{7}$$

by using total width of the slot conductors b_C and slot width b_S. The decomposition into real and imaginary parts yields

$$k_{pR}(\xi) = \frac{\operatorname{Re} Z(\zeta)}{R_0} = \varphi_R(\xi) + p\,(p-1)\,\psi_R(\xi) \ , \tag{8a}$$

$$k_{pX}(\xi) = \frac{\operatorname{Im} Z(\zeta)}{\omega L_0} = \varphi_X(\xi) + p\,(p-1)\,\psi_X(\xi) \ , \tag{8b}$$

with the real functions

$$\varphi_R(\xi) = \xi\,\frac{\sinh 2\xi + \sin 2\xi}{\cosh 2\xi - \cos 2\xi} \ , \tag{9a}$$

$$\psi_R(\xi) = 2\xi\,\frac{\sinh\xi - \sin\xi}{\cosh\xi + \cos\xi} \ , \tag{9b}$$

$$\varphi_X(\xi) = \frac{3}{2\xi}\,\frac{\sinh 2\xi - \sin 2\xi}{\cosh 2\xi - \cos 2\xi} \ , \tag{9c}$$

$$\psi_X(\xi) = \frac{3}{\xi}\,\frac{\sinh\xi + \sin\xi}{\cosh\xi + \cos\xi} \ . \tag{9d}$$

In dependence on the arrangement of the slot conductors with the end winding connection, averaged values of resistance and inductance are described as

$$k_{nR}(\xi) = \varphi_R(\xi) + m(n)\,\psi_R(\xi) \ , \tag{10a}$$

$$k_{nX}(\xi) = \frac{1}{n^2}\left(\varphi_X(\xi) + m(n)\,\psi_X(\xi)\right) \ . \tag{10b}$$

Therein, weighting factors

$$m(n) = \frac{n^2-1}{3} \ , \quad m(n) = \frac{n^2-4}{6} \tag{11}$$

are introduced without or with transposition of the $n/2$ slot conductors in each layer, respectively [4].

In particular with the stator, the current displacement within the end winding region has to be considered. According to [3], [4], the modified reduced conductor height

$$\xi' = \frac{h_C}{\delta_C}\sqrt{\frac{b_C}{b_C + 0.6\,n\,h_C}} \tag{12}$$

and modified weighting factor

$$m'(n) = \frac{n^2 - 4}{12} \tag{13}$$

define the averaged values of resistance and inductance as

$$k'_{nR}(\xi') = \varphi_R(\xi') + m'(n)\,\psi_R(\xi') \ , \tag{14a}$$

$$k'_{nX}(\xi') = \frac{4}{n^2}\Big(\varphi_X(\xi') + m'(n)\,\psi_X(\xi')\Big) \ . \tag{14b}$$

Finally, averaged resistance and inductance factors are obtained from

$$k_R(\xi) = \frac{k_{nR}(\xi)\,l_S + k'_{nR}(\xi)\,(l_W - l_S)}{l_W} \ , \tag{15a}$$

$$k_X(\xi) = \frac{k_{nX}(\xi)\,l_S + k'_{nX}(\xi)\,(l_W - l_S)}{l_W} \ , \tag{15b}$$

wherein l_S and l_W denote stacking length and half total length of one single winding, respectively.

B. Semi-closed rotor slots

In most cases, asynchronous induction machines of traction drives are equipped with unskewed semi-closed rotor slots containing rectangular or slightly trapezoidal slot conductors. By using the DC resistance R_0, the complex impedance of such slot conductors is given by

$$\frac{Z(\zeta)}{R_0} = \zeta^2\left(\frac{\coth\zeta}{\zeta} + \sum_{n=1}^{\infty} 2\left(\mathrm{si}\,\frac{n\pi s}{b_C}\right)^2 \frac{\coth\zeta_n}{\zeta_n}\right) \ , \tag{16}$$

$$\zeta_n = \sqrt{\left(\frac{2n\pi h_C}{b_C}\right)^2 + \zeta^2} \ ,$$

where s, b_C, h_C denote width of the slot opening as well as width and height of the conductor, respectively [6].

In case of unskewed semi-closed rotor slots containing cylindrical slot conductors, the complex impedance of the slot conductors is obtained from

$$\frac{Z(\zeta)}{R_0} = \frac{\zeta}{2}\left(\frac{I_0(\zeta)}{I'_0(\zeta)} + \sum_{n=1}^{\infty} 2\Big(\mathrm{si}\big(n\alpha\big)\Big)^2 \frac{I_n(\zeta)}{I'_n(\zeta)}\right) \ , \tag{17}$$

$$\alpha = \arcsin\frac{s}{2r_C} \ ,$$

wherein s, r_C denote width of the slot opening as well as radius of the slot conductor and I_n, I'_n are the modified Bessel functions of first kind and their derivates, respectively [6].

With respect to the additional losses of the higher harmonics, the impact of various designs of the end winding region can be neglected.

IV. Iron Losses

Another important component of the additional losses concerned arises as iron losses caused by the higher voltage harmonics in particular in the stator and less significantly in the rotor laminations [3]–[5].

Basically, iron losses can be separated into three contributions of eddy current losses P_{ec}, hysteresis losses P_{hy} and excess losses P_{ex} [9]–[13]. Each of these three iron loss densities has its own dependence on frequency and magnetic flux.

$$\text{Eddy current losses:} \quad p_{ec} \sim f_k^2\left(\frac{U_k}{f_k}\right)^2 \ ,$$

$$\text{Hysteresis losses:} \quad p_{hy} \sim f_k\left(\frac{U_k}{f_k}\right)^2 \ ,$$

$$\text{Excess losses:} \quad p_{ex} \sim f_k^{1.5}\left(\frac{U_k}{f_k}\right)^{1.5} \ .$$

In particular, the hysteresis losses are additionally influenced by the level of saturation caused by the fundamental harmonics when operating in either constant field or field weakening region [12], [13].

The magnetizing inductance of the fundamental harmonics can be evaluated in accordance with the magnetic characteristic of the entire machine for each operating point in either the constant field or field weakening region. Additionally, the saturation caused by the fundamental harmonics defines an appropriate differential magnetizing inductance representing the magnetization current of the higher harmonics.

The actual values of the iron losses are obtained from the geometry data as well as material dependent coefficients known from already utilized lamination sheets. According to four main iron regions as stator teeth and yoke as well as rotor teeth and yoke, the total iron losses of these regions are evaluated from the above power loss densities and the iron masses of the respective regions.

V. Comparison with Measurements

Fig. 3 and Fig. 4 depict a comparison of measurement and simulation data for the phase voltage with a synchronous mode operation of the inverter. Fig. 5 and Fig. 6 depict a comparison of measurement and simulation data for phase voltage and phase current with the block mode operation of the inverter arising with high fundamental frequencies in the field weakening range. Obviously, the presented approximation by using an equivalent circuit for each harmonic component can represent the behaviour of these higher harmonics in an appropriate way.

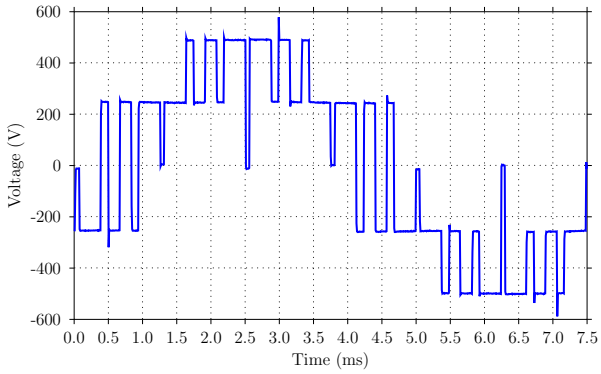

Fig. 3: Phase voltage with synchronous mode operation, measurement data

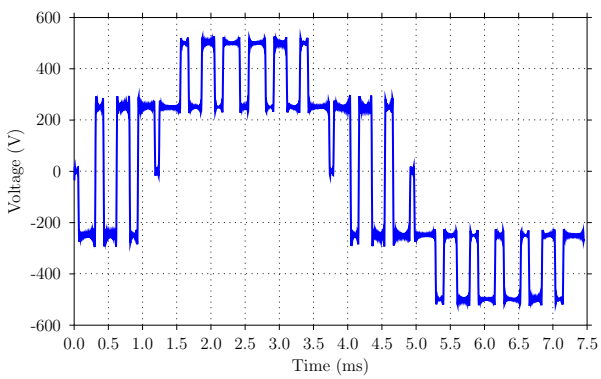

Fig. 4: Phase voltage with synchronous mode operation, simulation data

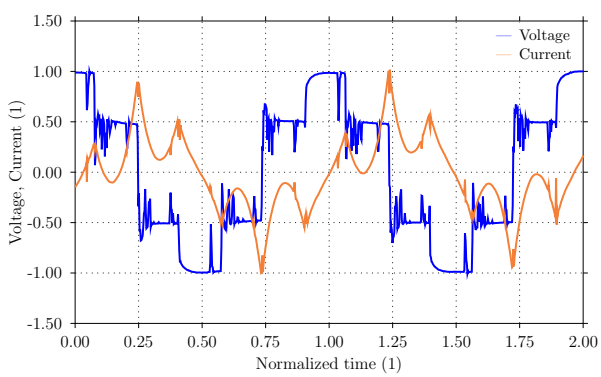

Fig. 5: Phase voltage and phase current with block mode operation, measurement data

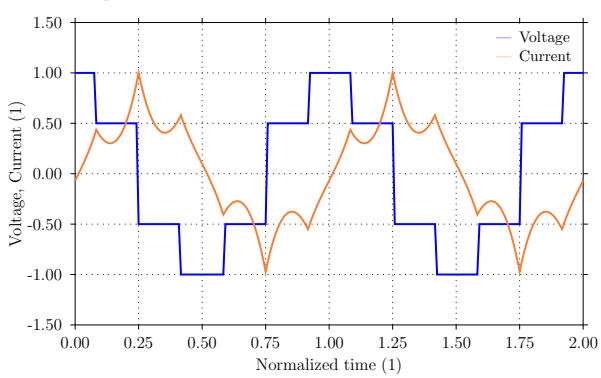

Fig. 6: Phase voltage and phase current with block mode operation, simulation data

Fig. 7 and Fig. 8 depict the measurement data for the additional losses caused by the inverter for a typical traction machine in dependence on the switching frequency of the inverter with different values of the DC link voltage.

Accordingly, Fig. 9, Fig. 10 and Fig. 11, Fig. 12 depict the simulation data for the additional losses caused by the inverter with different switching frequencies of the inverter as well as different values of the DC link voltage.

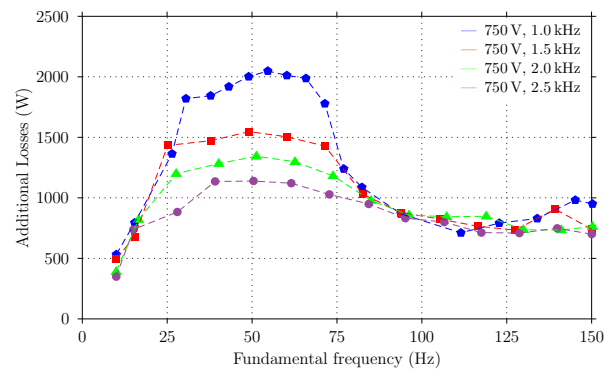

Fig. 7: Measurement data of additional losses caused by the inverter for an asynchronous induction machine of traction drives with a rated power of 100 kW in dependence on the switching frequency, DC link voltage of 750 V

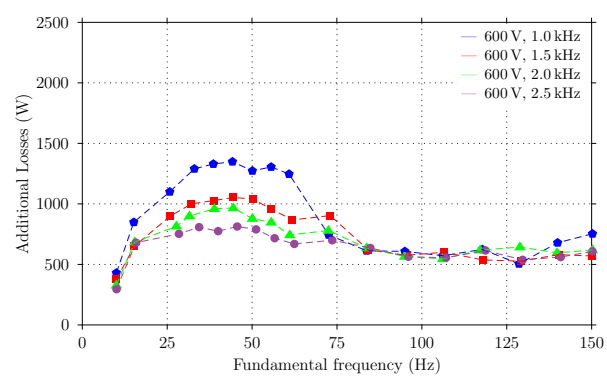

Fig. 8: Measurement data of additional losses caused by the inverter for an asynchronous induction machine of traction drives with a rated power of 100 kW in dependence on the switching frequency, DC link voltage of 600 V

As obtained from measurements, the switching frequency of the inverter significantly affects the total additional losses caused by the higher harmonic components. On the other hand, an increased switching frequency of the inverter causes additional losses and subsequently thermal design problems with the inverter. But an increased switching frequency of the inverter yields decreased additional losses in particular in the constant field region. In the field weakening range, the switching frequency of the inverter affects the additional losses only slightly. Additionally, the DC link voltage strongly influences the to-

tal additional losses caused by the higher harmonic components since these losses depends on the DC link voltage approximately quadratic.

The comparison with the evaluated data obtained from equivalent circuits of the higher harmonics shows a good accordance. As expected, the most dominant part of the additional losses caused by the higher harmonics arises from the power losses within the rotor. All three main components of the additional losses increase with fundamental frequencies up to values approximately to the half of the constant field region. With higher fundamental frequencies in the upper constant field region, they decrease to smaller values. Finally, all three portions are approximately constant within the field weakening region.

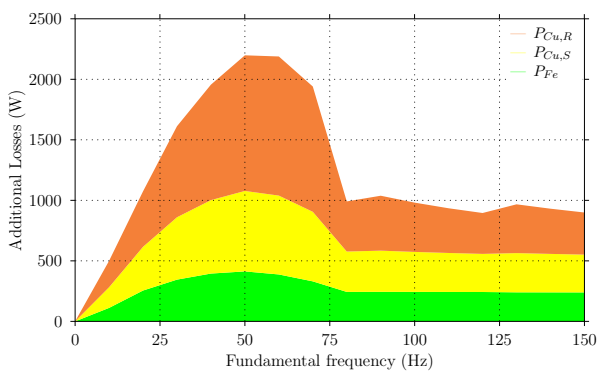

Fig. 9: Simulated main components of additional losses caused by the inverter for an asynchronous induction machine of traction drives with a rated power of 100 kW, switching frequency of 1 kHz, DC link voltage of 750 V

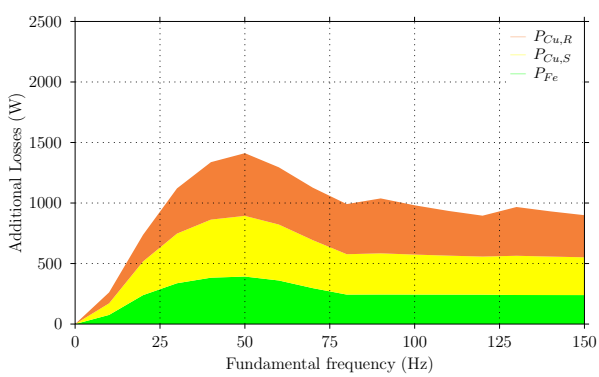

Fig. 10: Simulated main components of additional losses caused by the inverter for an asynchronous induction machine of traction drives with a rated power of 100 kW, switching frequency of 2 kHz, DC link voltage of 750 V

Consequently, there are important fields of an optimization of both electrical machine and inverter in order to get an optimal behaviour of both components in terms of losses and efficiency. In order to reduce the additional losses caused by the inverter, in particular switching mode as well as DC link voltage of the inverter should be selected for each application separately.

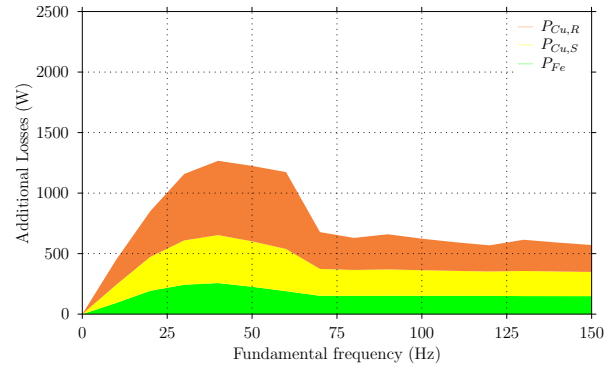

Fig. 11: Simulated main components of additional losses caused by the inverter for an asynchronous induction machine of traction drives with a rated power of 100 kW, switching frequency of 1 kHz, DC link voltage of 600 V

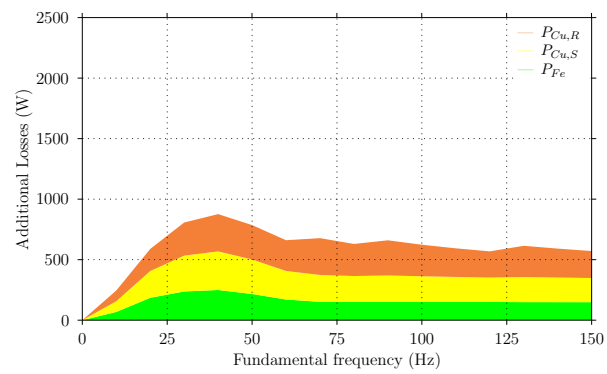

Fig. 12: Simulated main components of additional losses caused by the inverter for an asynchronous induction machine of traction drives with a rated power of 100 kW, switching frequency of 2 kHz, DC link voltage of 600 V

VI. Conclusion

In terms of additional losses caused by non-sinusoidal voltages and currents of the supplying voltage source inverter, asynchronous induction machines used with traction drives of rail transportation vehicles have to be treated differently than standard induction machines. Therefore, the paper discusses modelling and precalculation of power and iron losses additionally arising from the inverter to be suitable for a more accurate initial design of such machines.

Special attention is paid to an inclusion of various components of the iron losses as well as an accurate evaluation of the current displacement and the subsequent additional power losses in both stator and rotor slot conductors including the end winding regions. The presented evaluation method based on Fourier analyses of the terminal voltages is successfully

compared with detailed measurement results obtained from already built machines.

References

[1] Kleinrath H.: *Stromrichtergespeiste Drehfeldmaschinen* (in German). Springer, Vienna, 1980.

[2] Beaty H.W., Kirtley J.L.: *Electric Motor Handbook*. McGraw-Hill Book Company, New York (USA), 1998.

[3] Pyrhönen J., Jokinen T., Hrabovcová V.: *Design of Rotating Electrical Machines*. John Wiley & Sons Ltd, Chicester (UK), 2008.

[4] Müller G., Vogt K., Ponick B.: *Berechnung elektrischer Maschinen* (in German). Wiley-VCH, Weinheim, 2008.

[5] Green T.C., Hernandez-Aramburo C.A., Smith A.C.: "Losses in Grid and Inverter Supplied Induction Machine Drives". *IEE Proceedings Electrical Power Applications*, Vol. 150, No. 6, November 2003.

[6] Schmidt E.: *Stromverdrängung in Nutenleitern* (in German). Master Thesis, Vienna University of Technology, 1985.

[7] Islam M.J., Arkkio A.: "Effects of Pulse-Width Modulated Supply Voltage on Eddy Currents in the Form-Wound Stator Winding of a Cage Induction Motor". *IET Electric Power Applications*, Vol. 3, No. 1, January 2009.

[8] Islam M.J., Khang H.V., Repo A.K., Arkkio A.: "Eddy Current Loss and Temperature Rise in the Form-Wound Stator Winding of an Inverter Fed Cage Induction Motor". *IEEE Transactions on Magnetics*, Vol. 46, No. 8, August 2010.

[9] Boglietti A., Bottauscio O., Chiampi M., Pastorelli M., Repetto M.: "Computation and Measurement of Iron Losses under PWM supply conditions". *IEEE Transactions on Magnetics*, Vol. 34, No. 4, July 1998.

[10] Boglietti A., Chiampi M., Repetto M., Bottauscio O., Chiarabaglio D.: "Loss Separation Analysis in Ferromagnetic Sheets Under PWM Inverter Supply". *IEEE Transactions on Magnetics*, Vol. 34, No. 4, July 1998.

[11] Pippuri J., Arkkio A.: "Time-Harmonic Induction Machine Model Including Hysteresis and Eddy Currents in Steel Laminations". *IEEE Transactions on Magnetics*, Vol. 45, No. 7, July 2009.

[12] Dlala E., Arkkio A.: "A General Model for Investigating the Effects of the Frequency Converter on the Magnetic Iron Losses of a Squirrel-Cage Induction Motor". *IEEE Transactions on Magnetics*, Vol. 45, No. 9, September 2009.

[13] Boglietti A., Cavagnino A., Ionel D.M., Popescu M., Staton D.A., Vaschetto S.: "A General Model to Predict the Iron Losses in PWM Inverter-Fed Induction Motors". *IEEE Transactions on Industry Applications*, Vol. 46, No. 5, September 2010.